Basic Res Cardiol (2016)111:6
DOI 10.1007/s00395-015-0522-5

ORIGINAL CONTRIBUTION

Knock-out of nexilin in mice leads to dilated cardiomyopathy and endomyocardial fibroelastosis

Zouhair Aherrahrou[1,2,3] · Saskia Schlossarek[2,4] · Stephanie Stoelting[1,2] · Matthias Klinger[5] · Birgit Geertz[2,4] · Florian Weinberger[2,4] · Thorsten Kessler[6] · Redouane Aherrahrou[1,2] · Kristin Moreth[7] · Raffi Bekeredjian[8] · Martin Hrabě de Angelis[7,9,10] · Steffen Just[11] · Wolfgang Rottbauer[11] · Thomas Eschenhagen[2,4] · Heribert Schunkert[6,12] · Lucie Carrier[2,4] · Jeanette Erdmann[1,2,3]

Received: 13 January 2015 / Accepted: 19 November 2015

Abstract Cardiomyopathy is one of the most common causes of chronic heart failure worldwide. Mutations in the gene encoding nexilin (NEXN) occur in patients with both hypertrophic and dilated cardiomyopathy (DCM); however, little is known about the pathophysiological mechanisms and relevance of NEXN to these disorders. Here, we evaluated the functional role of NEXN using a constitutive *Nexn* knock-out (KO) mouse model. Heterozygous (Het) mice were inter-crossed to produce wild-type (WT), Het, and homozygous KO mice. At birth, 32, 46, and 22 % of the mice were WT, Het, and KO, respectively, which is close to the expected Mendelian ratio. After postnatal day 6, the survival of the *Nexn* KO mice decreased dramatically and all of the animals died by day 8. Phenotypic characterizations of the WT and KO mice were performed at postnatal days 1, 2, 4, and 6. At birth, the relative heart weights of the WT and KO mice were similar; however, at day 4, the relative heart weight of the KO group was 2.3-fold higher than of the WT group. In addition, the KO mice developed rapidly progressive cardiomyopathy with left ventricular dilation and wall thinning and decreased cardiac function. At day 6, the KO mice developed a fulminant DCM phenotype characterized by dilated ventricular chambers and systolic dysfunction. At this stage, collagen deposits and some elastin deposits were observed within the left ventricle cavity, which resembles the features of endomyocardial fibroelastosis (EFE). Overall, these results further emphasize the role of NEXN in DCM and suggest a novel role in EFE.

Electronic supplementary material The online version of this article (doi:10.1007/s00395-015-0522-5) contains supplementary material, which is available to authorized users.

✉ Zouhair Aherrahrou
zouhair.aherrahrou@iieg.uni-luebeck.de

[1] Institute for Integrative and Experimental Genomics, University of Lübeck, 23562 Lübeck, Germany

[2] DZHK (German Research Centre for Cardiovascular Research), partner site Hamburg/Lübeck/Kiel, Lübeck/Hamburg, Germany

[3] University Heart Center Luebeck, 23562 Lübeck, Germany

[4] Department of Experimental Pharmacology and Toxicology, Cardiovascular Research Center, University Medical Center Hamburg-Eppendorf, Hamburg, Germany

[5] Institute for Anatomy, University of Lübeck, Lübeck, Germany

[6] Deutsches Herzzentrum München, Klinik für Herz- und Kreislauferkrankungen, Technische Universität München, Munich, Germany

[7] German Mouse Clinic, Institute of Experimental Genetics, Helmholtz Zentrum München, German Research Center for Environmental Health, Ingolstaedter Landstrasse 1, 85764 Neuherberg, Germany

[8] Department of Cardiology, University of Heidelberg, Im Neuenheimer Feld 410, 69120 Heidelberg, Germany

[9] Chair of Experimental Genetics, School of Life Science Weihenstephan, Technische Universität München, Alte Akademie 8, 85354 Freising, Germany

[10] German Center for Diabetes Research (DZD), Ingostädter Landstr. 1, 85764 Neuherberg, Germany

[11] Department of Internal Medicine II, University Hospital Ulm, Ulm, Germany

[12] DZHK (German Research Centre for Cardiovascular Research), partner site Munich Heart Alliance (MHA), Munich, Germany

Published online: 10 December 2015

Keywords Dilated cardiomyopathy · Heart failure · Endocardial fibroelastosis · Nexilin · Knock-out mice

Introduction

Cardiomyopathies, which are among the leading causes of heart failure, can be divided into four idiosyncratic entities, namely dilated cardiomyopathy (DCM), hypertrophic cardiomyopathy (HCM), arrhythmogenic right ventricular cardiomyopathy, and restrictive cardiomyopathy [8, 29]. DCM is usually a late onset disease [26] that occurs at the age of 40–60 years, although it can also occur in the fetal period, infancy, early or late childhood, adolescence, and the elderly [4]. The disease is characterized by a progressive dilation of the ventricular chambers, accompanied by wall thinning and systolic dysfunction, which cause dyspnea, a poor quality of life, and a reduced life expectancy [7]. Myocardial damage can either be acquired due to immunological disease or toxicant abuse, or inborn due to mutations in a wide range of genes [2, 6, 24].

To date, several hundred mutations in more than 30 genes have been identified as being associated with sporadic and familial DCM; in fact, these mutations account for approximately 30–35 % of familial DCM cases [16, 17]. In most of these patients, DCM is inherited in an autosomal-dominant manner; however, autosomal-recessive and X-chromosomal inheritance patterns have been described in rare cases [22, 25]. Genetic studies revealed that, although the genes encoding sarcomeric proteins play the most important role in the pathophysiology of DCM, mutations in cytoskeletal, nuclear membrane, dystrophin-associated glycoprotein complex, and desmosomal proteins are also important causes of the disease [12, 13]. The sarcomere is the contractile unit of cardiac and skeletal muscle cells; its structure consists of a well-described alternate organization of thin and thick filaments, motor proteins such as myosin, and anchoring structures such as the Z-disc [3, 9]. Recently, the Z-disc has come to prominence as an important structural link between the cytoskeleton and the sarcolemma, as well as a nodal point in cardiomyocyte signal transduction [11].

In our previous study, we identified loss-of-function mutations in the gene encoding nexilin (NEXN) in patients with DCM [15]; all of these patients were heterozygous (Het) carriers of the *NEXN* mutations. The identified *NEXN* mutations included a deletion of three base pairs encoding a glycine residue at position 650, and two missense mutations at positions 1831 and 1955 (p.C1831A and p.A1955G). None of the identified mutations were found in the control cohorts. Very recently, ten mutations within the coding region of the *NEXN* gene were identified in 639 DCM patients using next-generation sequencing [14]; these mutations include p.E110Q, p.G157V, p.G245R, p.E332A, p.T363R, p.R392*, p.E468del, p.E470Q, p.E485K, and p.T666A.

Functional analyses using a zebrafish model demonstrated the important role of NEXN in dilation of the atrium and ventricle, which leads to severe heart failure with reduced systolic function. Electron microscopy analyses showed that the absence of NEXN disrupts the sarcomere integrity and Z-disc architecture severely in both zebrafish and patients carrying *NEXN* mutations [15], suggesting that NEXN dysfunction plays a pivotal role in DCM. Notably, Wang and colleagues identified loss-of-function mutations in the *NEXN* gene in two probands exhibiting HCM [32]. In this respect, *NEXN* has joined the growing list of genes whose mutations lead to either DCM or HCM [15, 32].

To date, the functional role of NEXN in DCM has only been demonstrated using a zebrafish model [15]; to understand this role fully, the anatomical and physiological differences between heart development in zebrafish and mammals must be considered [21, 27]. Here, to gain a more in-depth insight into the pathophysiology of NEXN in DCM, we generated a constitutive *Nexn* knock-out (KO) mouse model and characterized the cardiac disorders of the mice.

Materials and methods

Generation and genotyping of Nexn KO mice

A *Nexn* targeting construct was designed to insert a neomycin selection cassette and two *loxP* sites flanking exons 2 and 4 of the mouse *Nexn* gene (Fig. 1a). Gene targeting was performed in 2066 A-F9 embryonic stem cells and the targeted clones were microinjected into C57BL/6N blastocysts. Targeted recombinants were verified by Southern blot analysis after digestion with appropriate restriction enzymes for the targeted (KO) and wild-type (WT) alleles (Artemis). Gt(ROSA)26Sortm16(cre)^{Arte} were crossed to the floxed mice to generate the conventional Knockout for *Nexn*. The generated Het mice were produced and genotyped via PCR analyses of DNA samples isolated from ear biopsies. The PCR products were amplified using Eppendorf® MasterMix (2.5×), according to the manufacturer's instructions. The following primers were used to amplify the PCR fragments shown in Fig. 1a, b: *Nexn*-1, 5′-GTCTACTGAGTAAGTCCACAG-3′; *Nexn*-2, 5́-GAGAACTAATCAGGATGTTGC-3′; and *Nexn*-3, 5′-TCCCAGCAGAGGTTATTTGC-3′. *Nexn*-1 and -3 were designed to generate PCR fragments of 361 bp for the KO allele and 3934 bp for the WT allele, the latter of which was not

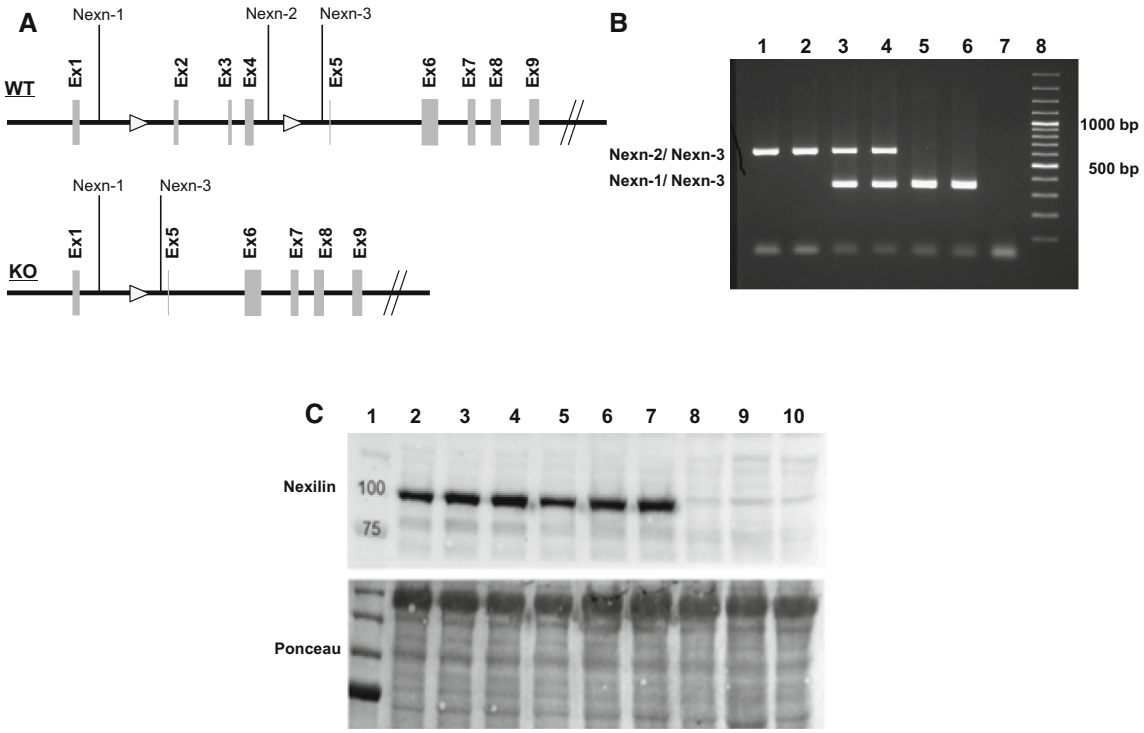

Fig. 1 Generation of *Nexn* KO mice and confirmation of NEXN deficiency at the DNA and protein level. **a** The targeting construct that was designed to insert *loxP* sites flanking exons 2 and 4 of the mouse *Nexn* gene. **b** Genotyping of mice using Nexn-1 and -3 produced a 361 bp band from the KO mice (mutated allele), and genotyping using Nexn-2 and -3 produced a 629 bp band from the WT allele. Samples *1* and *2*, *3* and *4*, and *5* and *6* correspond to the WT, Het, and KO mice, respectively. Samples *7* and *8* correspond to H_2O and the DNA ladder, respectively. **c** Western blot analysis demonstrating the absence of NEXN protein in the KO mice. Samples *2–4*, *5–7*, and *8–10* correspond to the WT, Het, and KO mice, respectively. Sample 1 corresponds to the molecular weight marker

amplified due to its large size. To discriminate between Het (WT/KO) and homozygous KO (KO/KO) mice, *Nexn*-2 and -3 were designed to produce a 629 bp fragment for the WT allele only.

Confirmation of NEXN deficiency via Western blotting

Hearts were excised from the newborn mice, mixed with five volumes of lysis buffer (3 % sodium dodecyl sulfate, 30 mM Tris base (pH 8.8), 5 mM ethylenediaminetetraacetic acid, 30 mM NaF, and 10 % glycerol), and homogenized twice with a Tissue Lyser (Qiagen) for 30 s at 20 Hz. The insoluble material was removed by centrifuging the samples at 13,200 rpm for 10 min at 20 °C, and the protein concentrations of the supernatants were determined using Bio-Rad protein assay reagent. Proteins were loaded onto acrylamide/bisacrylamide (29:1) gels and electrotransferred to nitrocellulose membranes (0.45 µm pore size). The membranes were stained overnight at 4 °C with a monoclonal antibody against NEXN (Sigma, 1:5000). After incubation with a mouse horseradish peroxidase-conjugated secondary antibody (Dianova, 1:20,000) at room temperature for 1 h, the signal was revealed using ECL Plus reagent (Amersham) and detected using the Chemi Genius Bio Imaging System.

Macroscopic and microscopic examination

All animal studies were conducted in accordance with the local animal welfare committees of Schleswig–Holstein, Hamburg and Bavaria, Germany.

Hearts were collected from mice at postnatal days 1, 2, 4, and 6. The animals underwent macroscopic examination as well as histologic analyses. The heart weight to body weight ratios (relative heart weights) were determined for each mouse and histological analyses were performed following complete dissection. The hearts were fixed in 4 % formaldehyde and embedded in paraffin. Sections of the tissues (4–6 µm thick) were stained with standard hematoxylin and eosin (H&E) for histologic evaluation. Masson's Trichrome and Sirius Red staining were used to detect collagen fibers, and Verhoeff-Van Gieson (VVG) staining was used to detect elastin fibers.

Transmission electron microscopy

For transmission electron microscopy (TEM), hearts from newborn mice were collected, fixed in 2.5 % glutaraldehyde and 2.0 % paraformaldehyde in cacodylate buffer (pH 7.4), and then post-fixed in 2.0 % osmium tetroxide solution. The samples were transferred through graded ethanol concentrations to eliminate water, and then embedded in propylene oxide. Ultra-thin Sections (40–60 nm thick) were cut, stained with lead citrate and uranyl acetate, and examined with an EM400 transmission electron microscope.

Echocardiographic analysis

Transthoracic echocardiography was performed using the Vevo 2100 System (VisualSonics). For the cohort of 3 months old heterozygotes and respective controls analyzed in the German Mouse Clinic, the Vevo 770 System with RMV-707 transducer was used. The animals were anesthetized with isoflurane (0.8–1.0 %) and secured to a warming platform in a supine position. B-mode images were obtained using a MS550 transducer and images were obtained in the parasternal short and long axis view. The dimensions of the left ventricle (thickness of the anterior and posterior walls, as well as the left ventricular diameter) were measured in the short axis view during both diastole and systole.

Reverse transcription and qPCR

Total RNA was extracted from myocardial tissue at postnatal days 0, 1, and 6 using Qiagen kits. The RNA was reverse-transcribed into complementary DNA as described previously [1], and the transcript levels in KO mice were related to those in age-matched WT mice. The following forward and reverse primer sequences were used for qPCR amplifications: skeletal α-actin (*Acta1*), 5′-CCC CTG AGG AGC ACC CGA CT-3′ and 5′-CGT TGT GGG TGA CAC CGT CCC-3′; β-myosin heavy chain (*Myh7*), 5′-GAG GAG AGG GCG GAC ATC-3′ and 5′-GGA GCT GGG TAG CAC AAG AG-3′; atrial natriuretic peptide (*Nppa*), 5′-TGA AAA GCA AAC TGA GGG CT-3′ and 5′-CAG AGT GGG AGA GGC AAG AC-3′; and elastin (*Eln*), 5′-CGG TGT TGG TGG TAT TGG T-3′ and 5′-GCT TTG ACT CCT GTG CCA GT-3′. The expression level of glyceraldehyde-3-phosphate dehydrogenase (*Gapdh*: 5′-GAC CAC AGT CCA TGC CAT CAC-3′ and 5′-CCG TTC AGC TCT GGG ATG AC-3′) was used as an internal standard.

Statistical analysis

Data are presented as the mean ± SEM. To examine the differences between the relative heart weights of the WT and NEXN KO mice, unpaired *t* tests were performed using StatView Software version 5.0.1. A one-way ANOVA followed by Dunnett's post test was used to analyze the echocardiographic data. For the cohort of 3 months old heterozygotes and respective controls a one-way ANOVA was used. $P < 0.05$ was considered statistically significant. For all tests, $*P < 0.05$, $**P < 0.01$, $***P < 0.001$, and n.s., not significant.

Results

Generation of Nexn KO mice

The Nexn KO mice were generated using a gene targeting strategy designed to delete the chromosomal fragment between exons 2 and 4 of *Nexn* (Fig. 1a). NEXN deficiency was confirmed at the genomic DNA and protein levels. At the DNA level, amplification of the fragment including exons 2 and 4 of the *Nexn* gene using *Nexn*-1 and 3 primers produced a short DNA fragment of 361 bp for the KO mice (Fig. 1b). The corresponding 3934 bp fragment for the WT mice could not be amplified due to its large size. The presence of the WT allele in WT and Het mice was confirmed by PCR amplification of a 629 bp fragment using *Nexn*-2 and *Nexn*-3, the former of which was complementary to the targeted region (Fig. 1a, b). In addition, Western blotting confirmed the absence of NEXN protein the KO hearts (Fig. 1c).

Nexn deficiency leads to early postnatal lethality

Adult Het mice were inter-crossed to produce WT, Het, and KO mice, and the survival rates of these three groups were determined between postnatal days 0 and 8 (Fig. 2a). At birth, 32, 46, and 22 % of the mice were WT, Het, and KO, respectively, which is close to the expected Mendelian ratio of 1:2:1 (Fig. 2b). After postnatal day 2, the survival of the KO mice decreased dramatically, as shown by a Kaplan–Meier curve (Fig. 2a). Of the 135 confirmed KO mice, 134 died within 8 days after birth (Fig. 2a).

Nexn deficient mice display increased heart weight and endomyocardial fibroelastosis

As mentioned above, the absence of NEXN led to premature mortality of KO mice and offered a narrow time frame for further investigations of the cardiac phenotype, which focused on the relative heart weight and histologic analyses. The *Nexn* KO mice appeared normal at birth and displayed no apparent cardiac pathology (Figs. 3a, 4, Day 1). However, after postnatal day 4, the relative heart weight was 2.3-fold higher in KO than in WT mice, and KO and WT hearts were visibly different at the macroscopic and

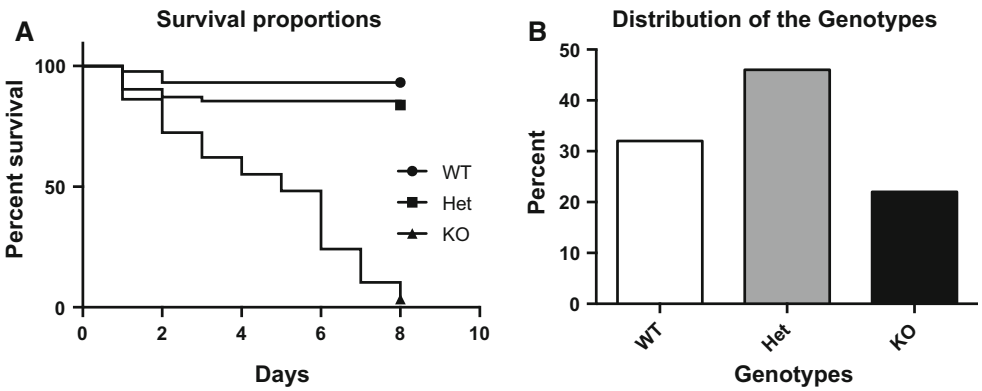

Fig. 2 Survival curve analysis and genotype distribution of the *Nexn* KO mice at birth. **a** Survival analysis of WT, Het, and KO mice on postnatal days 0–8. **b** The distributions of the WT, Het, and KO mice at postnatal day 5

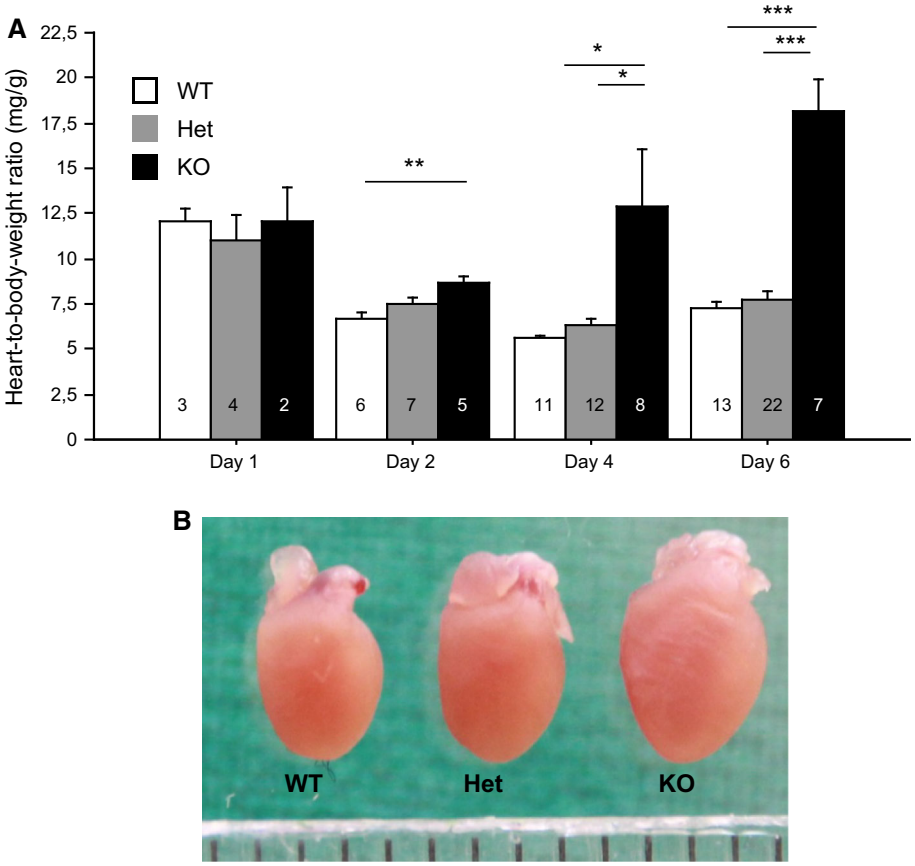

Fig. 3 Phenotypic characterization of the *Nexn* KO mice. **a** The relative heart weights of the *Nexn* WT, Het, and KO mice at postnatal days 1, 2, 4, and 6. **b** Representative macroscopic observation of hearts from the WT, Het, and KO mice at postnatal day 6, Number of animals are indicated in the *bars*. *Scale bar*, 1 mm

microscopic levels, particularly at postnatal day 6 (Figs. 3a, b, 4). The relative heart weights of Het and WT mice were comparable at all time-points examined (Fig. 3a). H&E staining of heart sections revealed that the KO mice had developed rapidly progressive left ventricular dilation and wall thinning at postnatal day 6 (Fig. 4). Endocardial deposits were also observed in KO mice at this time-point; to examine the composition of these deposits, different stains were used to detect collagen and elastin fibers. Trichrome staining demonstrated a high level of fibrosis with collagen deposits (Fig. 4, Day 6). Furthermore, VVG detected moderate elastin deposits at postnatal day 6 (Fig. 4, arrows). A few deposits were also detected in the right ventricle (data not shown). To gain more insights into the structure of EFE deposits, semi-thin sections from araldite-embedded tissues were used and stained with methylene blue/Azur II. Dramatic deposits within the inner ventricle chamber were observed (Fig. 5a).

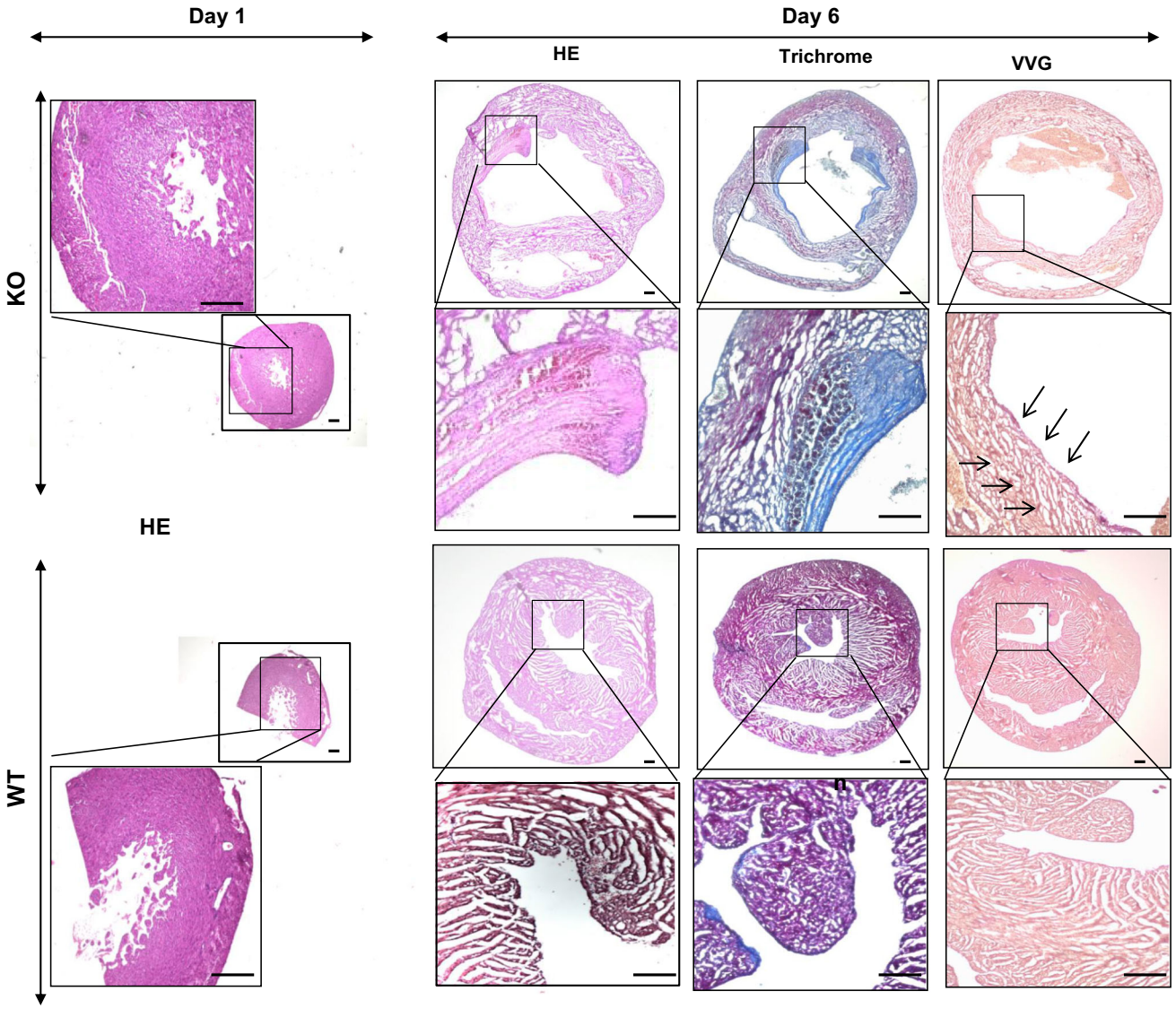

Fig. 4 Microscopic analyses of the hearts of *Nexn* KO mice. H&E, Trichrome, and VVG staining of hearts from the *Nexn* KO and WT mice at postnatal days 1 and 6 to identify strong collagen fibers (stained in *blue* using Trichrome) and moderate elastin (stained in *dark purple* using VVG) within the endomyocardial fibrotic deposits in the left ventricle. Ten mice in each group were analyzed and five mice were further taken for quantification. *Scale bar* 0.2 mm

KO sarcomeres are not affected

Next, TEM was used to evaluate the integrities of the sarcomere myofilaments and Z-disks in the *Nexn* KO and WT mice; however, no obvious abnormalities of these structures were identified in either group of mice (Fig. 5b).

KO and to a lesser extent Het mice developed dilated cardiomyopathy

To assess the cardiac phenotypes of the WT, Het, and KO mice, echocardiographic evaluations were performed at postnatal days 4–6 (Fig. 6). The anterior and posterior wall thickness in diastole were both lower in KO than in WT mice. The LV internal diameter in diastole and systole were higher, and the fractional area shortening was markedly lower in KO than in WT mice. LVM did not differ between groups. However LVM/BW was higher, mainly due to the lower BW in KO than in WT. Het mice also displayed a mild DCM phenotype with slight dilatation and reduced fractional shortening. Thus, there was a dose-dependent effect of the reduced level of NEXN on DCM at postnatal days 4–6. However, this effect was not seen in aging mice. Echocardiographic analysis of 3-month-old Het mice demonstrated no changes in heart morphology or function compared to WT mice (Suppl. Table).

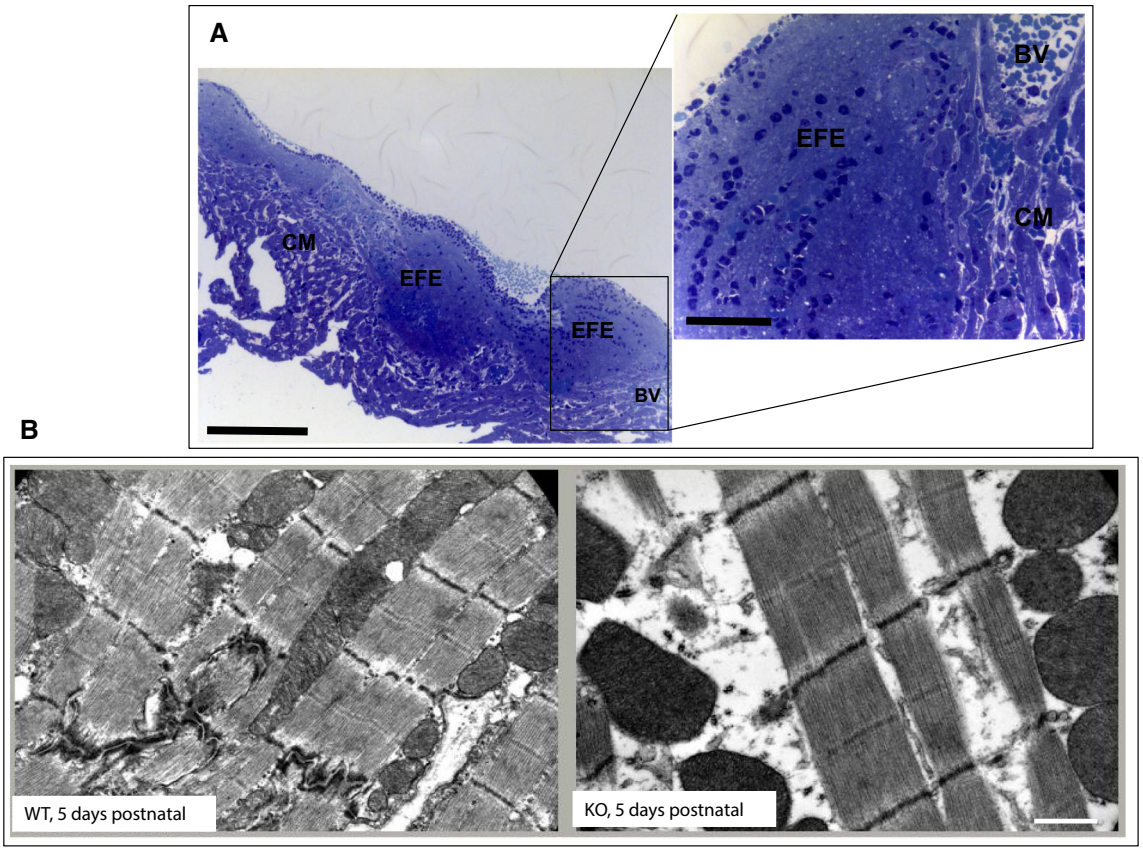

Fig. 5 Semithin section and TEM analyses. **a** Semithin section from araldite-embedded tissue, stained with methylene blue/Azur II. The wall of the left ventricle contains cardiomyocytes (CM), fibro-elastic deposits (FE) and blood vessels (BV). *Bars* 150 µm (overview) and 50 µm (inset). **b** The structures of sarcomeric myofilaments and particularly the Z-disks were further analyzed using TEM and display no differences between NEXN KO and WT mice. *Scale bar* 0.7 µm

Nexn deficiency in mice leads to increased expression of cardiomyopathy and endomyocardial fibroelastosis markers

The *Myh7*, *Acta1*, and *Nppa* mRNAs were selected as molecular markers of hypertrophy, and the *Eln* mRNA was selected as a molecular marker of endomyocardial fibroelastosis (EFE). RT-qPCR analyses revealed no changes in the expression of the hypertrophic markers in the KO mice compared to WT mice at birth. However, a slight increase was already observed for Eln at birth, which was 1.8-fold higher in KO than in WT mice (Fig. 7). At postnatal day 1 the expression level of *Myh7* was higher in the KO mice than the WT mice (Fig. 7), which was prior to the development of cardiomyopathy. The increase in *Myh7* as well as *Nppa* expression persisted until postnatal day 6 (Fig. 7). The normalization of the expression level of *Acta1* at day 6 strongly supports the DCM rather than hypertrophy phenotype (Fig. 7). Conversely the higher *Nppa* level at 6 days than 1 day also markedly supports the dysfunction. The expression level of *Eln* in the KO mice was also significantly higher than that in the WT mice at postnatal day 6.

Discussion

All forms of cardiomyopathy are serious clinical problems in Western countries and can lead to heart failure and require subsequent heart transplantation. In our previous study, we identified *NEXN* as a novel DCM-related gene and functionally studied its role in heart failure using a zebrafish model [15]. Here, we developed a *Nexn* KO mouse model to obtain a deeper understanding of the role of this protein in DCM in mammals.

The complete absence of NEXN led to premature death of the KO mice in a very narrow time frame (between postnatal days 6 and 8). Our previous study in zebrafish [15] revealed that NEXN is one of a number of structural proteins that are specifically localized in the Z-disc and play a key role in maintaining the integrities of the cytoskeleton and sarcomere. NEXN also plays an essential role in force transmission between sarcomeres and the sarcolemma. A previous immunohistological analysis demonstrated positive staining of NEXN at the Z-disc of the sarcomere, where it co-localized with alpha-actinin,

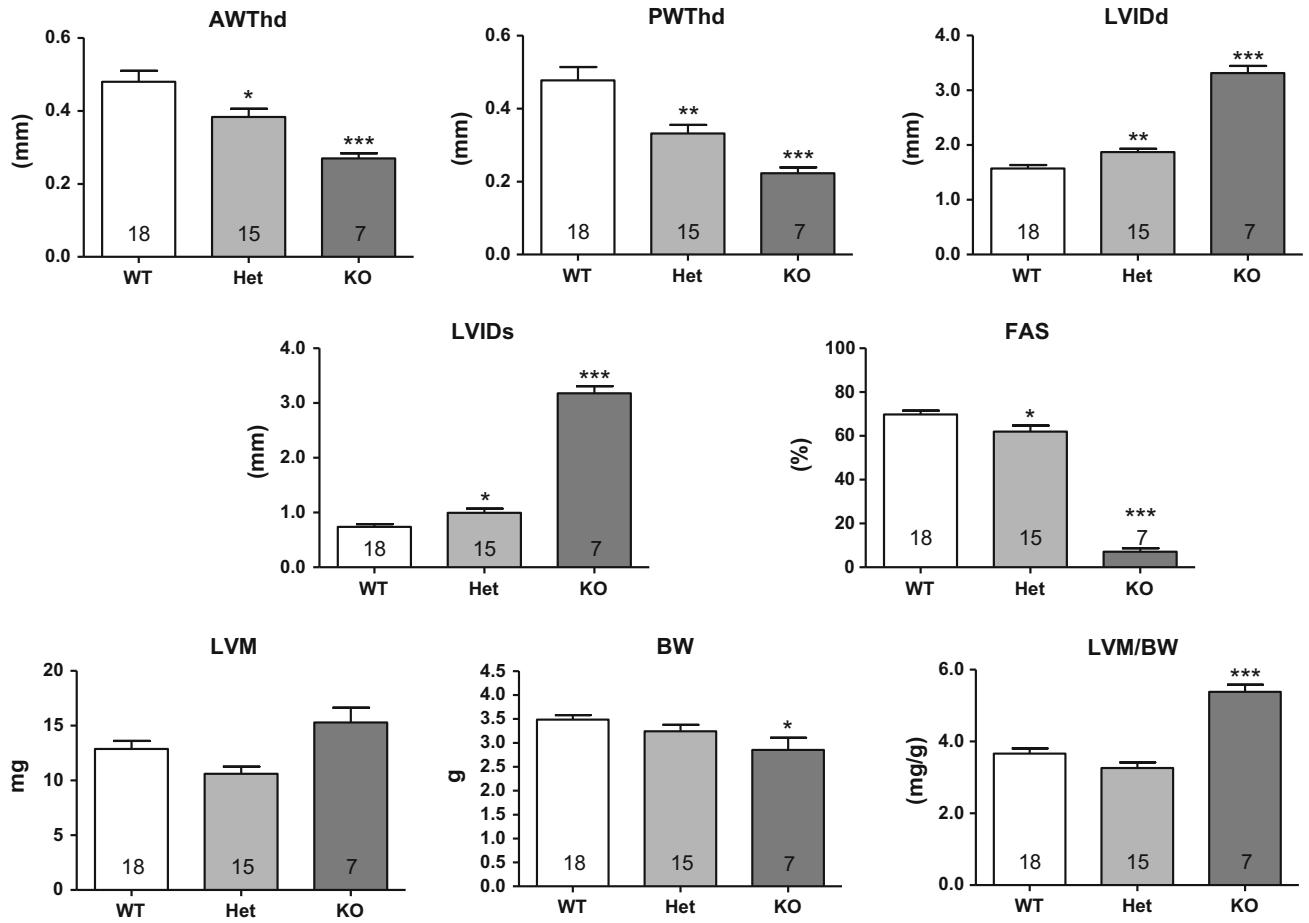

Fig. 6 Transthoracic echocardiography analyses of *Nexn* WT, Het, and KO mice. The analyses were performed in 4–6-day-old mice. Data are expressed as the mean ± SEM. $*P < 0.05$, $**P < 0.01$, and $***P < 0.001$ versus WT, using a one-way ANOVA plus Dunnett's post test. The numbers of animals examined are indicated in the *bars*. *LVM/BW* left ventricular mass to body weight ratio, *FAS* fractional area shortening, *AWThd* anterior wall thickness in diastole, *PWThd* posterior wall thickness in diastole, *LVIDd* left ventricular internal diameter in diastole, *LVIDs* left ventricular internal diameter in systole. Number of animals is indicated in the *bars*

thereby highlighting the key role of NEXN in the stabilization of sarcomeres [15]. As observed previously in humans and zebrafish, the *Nexn* KO mice displayed DCM at an early stage of heart development (postnatal day 4). Furthermore, the relative heart weight was 2.3-fold higher in the KO group than WT group, and the KO mice displayed rapid progressive cardiomyopathy with dilation and wall thinning and extremely reduced contractile function. At the molecular level, markers of DCM were expressed at higher levels in the KO mice than the WT mice. However, in contrast to the zebrafish model, the Z-disc in the *Nexn* KO mouse model remained stable and no obvious abnormalities were detected using TEM.

Notably, DCM progression in the *Nexn* KO mice was accompanied by EFE, a rare heart disorder characterized by thickening of the innermost lining of the heart chambers due to an increase in the amount of supporting connective tissue and elastic fibers [10]. To date, the pathogenesis of EFE has remained unclear, although the disorder is characterized by collagen and elastin fiber deposits in the endocardium. Here, we confirmed this finding by staining the KO hearts with Trichrome and VVG, which are specific for collagen and elastin deposits, respectively [19, 28]. In addition, we demonstrated that the expression level of the *Eln* gene was higher in the *Nexn* KO mice than the WT mice.

Until 2006, EFE was classified as a rare cardiomyopathy disorder [23, 31]; in fact, EFE was omitted from the most recent Heart Association cardiomyopathy classifications [31]. However, a previous study demonstrated that 25 % of all pediatric DCM cases examined also had EFE [31], indicating that this altogether rare condition occurs frequently in this subset of patients. Jiao and colleagues also reported 75 EFE cases in infants in China [18]. Pediatric EFE patients in particular have a severely restricted life expectancy and do not survive past 2 years [5]. Although various causes of EFE have been proposed, including viral exposure and environmental insult [20], the causal factors

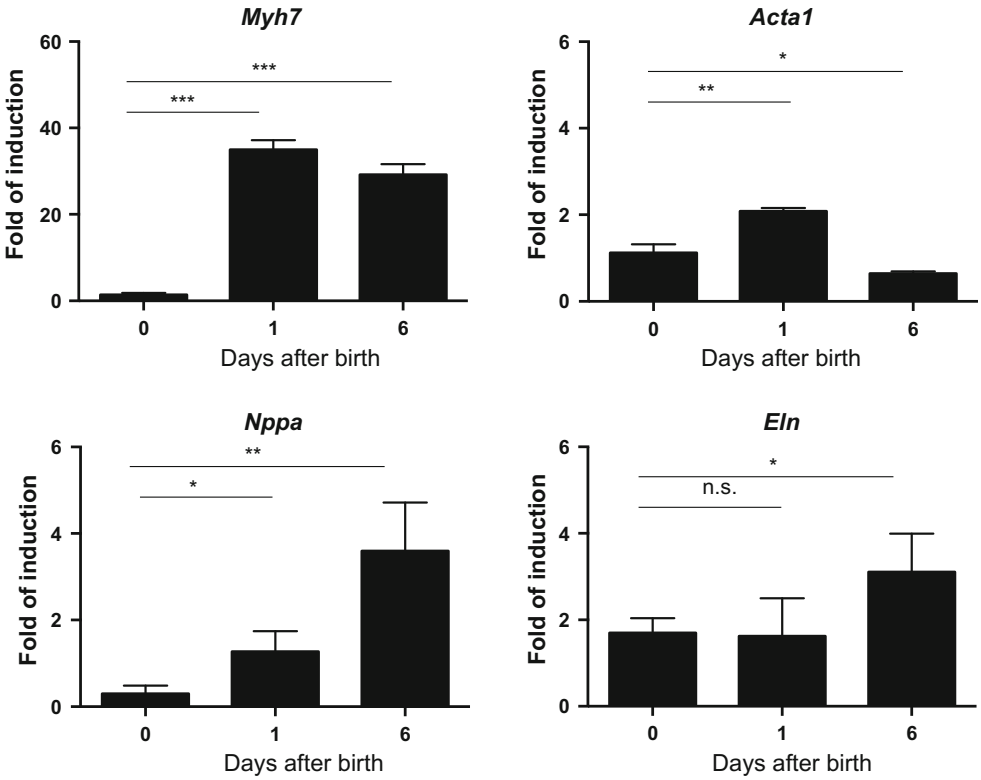

Fig. 7 RT-qPCR analyses of DCM and EFE markers. The expression levels of cardiomyopathy and EFE markers in the hearts of the WT and KO mice were performed at postnatal days 0, 1, and 6. The *bars* represent the gene expression levels relative to those in the WT mice. The data were obtained from three animals per group and three separate analyses. *Myh7* β-myosin heavy chain, *Nppa* atrial natriuretic peptide, *Acta1* skeletal α-actin, *Eln* elastin. Data are expressed as the mean ± SEM. $*P < 0.05$, $**P < 0.01$, and $***P < 0.001$ versus WT, using unpaired *t* test

are poorly understood. In addition, the genetic basis of EFE is unclear, but the disorder seems to be an important characteristic of an, until now, underestimated form of DCM. Only a few animal models of EFE, including cats, have been described to date [30]; here, we present a mouse model that may be used to better understand the pathogenesis of this underestimated fatal postnatal disorder and to clarify whether it is or is not a form of DCM.

The *Nexn* KO mice died between postnatal days 2 and 8, although it is unclear whether the cause of death was DCM or EFE. At this point, other causes cannot be excluded, but the extremely low ejection fraction makes heart failure a likely cause. Functional investigations of heart-specific conditional *Nexn* KO mice are required to gain new insights into the roles of NEXN in DCM and EFE. Furthermore, it is unclear whether mutations in *NEXN* are also associated with EFE, especially in pediatric patients. Overall, the results presented here highlight the role of NEXN in DCM and identify *Nexn* as a novel EFE-related gene in mice.

Acknowledgments We would like to thank Sandra Wrobel, Annett Liebers and Maren Behrensen for their technical support.

Compliance with ethical standards

Funding sources The generation and characterization of the Nexn KO mice was supported by grants from the Bundesministerium für Bildung und Forschung, NGFN and NGFN-plus and Infrafrontier grant (01KX1012) as well as from the DZHK (German Centre for Cardiovascular Research) and the German Ministry of Research and Education (BMBF). Furthermore the project was also supported by the Leducq Foundation (Research grant Nr. 11, CVD 04) and the Association Institut de Myologie (Paris). Current funding is provided by the German Federal Ministry of Education and Research (BMBF) in the context of the e:Med program (e:AtheroSysMed and sysINFLAME), the FP7 European Union project CVgenes@target (261123) and a grant from the Fondation Leducq (CADgenomics: Understanding Coronary Artery Disease Genes, 12CVD02. Further grants were received by the local focus program "Medizinische Genetik" of the Universität zu Lübeck. This study was also supported through the Deutsche Forschungsgemeinschaft (DFG) cluster of excellence 'Inflammation at Interfaces'.

Conflict of interest On behalf of all authors, the corresponding author states that there is no conflict of interest

References

1. Aherrahrou Z, Doehring LC, Kaczmarek PM, Liptau H, Ehlers EM, Pomarino A, Wrobel S, Gotz A, Mayer B, Erdmann J, Schunkert H (2007) Ultrafine mapping of Dyscalc1 to an 80-kb chromosomal segment on chromosome 7 in mice susceptible for dystrophic calcification. Physiol Genomics 28:203–212. doi:10.1152/physiolgenomics.00133.2006
2. Callis TE, Jensen BC, Weck KE, Willis MS (2010) Evolving molecular diagnostics for familial cardiomyopathies: at the heart of it all. Expert Rev Mol Diagn 10:329–351. doi:10.1586/erm.10.13
3. Clark KA, McElhinny AS, Beckerle MC, Gregorio CC (2002) Striated muscle cytoarchitecture: an intricate web of form and

function. Annu Rev Cell Dev Bi 18:637–706. doi:10.1146/annurev.cellbio.18.012502.105840
4. Colan SD, Lipshultz SE, Lowe AM, Sleeper LA, Messere J, Cox GF, Lurie PR, Orav EJ, Towbin JA (2007) Epidemiology and cause-specific outcome of hypertrophic cardiomyopathy in children: findings from the Pediatric Cardiomyopathy Registry. Circulation 115:773–781. doi:10.1161/CIRCULATIONAHA.106.621185
5. Cotran RS, Kumar V, Fausto N, Nelso F, Robbins SL, Abbas AK (2005). In: Robbins and Cotran (ed) Pathologic basis of disease, 8th edn. Saunders Elsevier, St. Louis, p 607
6. Doevendans PAWAA, Marcelis C, Doevendans PA, Bonne G (2001) Dilated cardiomyopathy in cardiovascular genetics for clinicians. Kluwer Academic Publishers, Dordrecht
7. Durand JB, Abchee AB, Roberts R (1995) Molecular and clinical aspects of inherited cardiomyopathies. Ann Med 27:311–317
8. Elliott P, Andersson B, Arbustini E, Bilinska Z, Cecchi F, Charron P, Dubourg O, Kuhl U, Maisch B, McKenna WJ, Monserrat L, Pankuweit S, Rapezzi C, Seferovic P, Tavazzi L, Keren A (2008) Classification of the cardiomyopathies: a position statement from the European Society Of Cardiology Working Group on Myocardial and Pericardial Diseases. Eur Heart J 29:270–276. doi:10.1093/eurheartj/ehm342
9. Ervasti JM (2000) Structure and function of the dystrophin-glycoprotein complex. madame curie bioscience database (Internet). Landes Bioscience, Austin
10. Fishbein MC, Ferrans VJ, Roberts WC (1977) Histologic and ultrastructural features of primary and secondary endocardial fibroelastosis. Arch Pathol Lab Med 101:49–54
11. Frank D, Frey N (2011) Cardiac Z-disc signaling network. J Biol Chem 286:9897–9904. doi:10.1074/jbc.R110.174268
12. Friedrich FW, Carrier L (2012) Genetics of hypertrophic and dilated cardiomyopathy. Curr Pharm Biotechno 13:2467–2476
13. Garcia-Pavia P, Cobo-Marcos M, Guzzo-Merello G, Gomez-Bueno M, Bornstein B, Lara-Pezzi E, Segovia J, Alonso-Pulpon L (2013) Genetics in dilated cardiomyopathy. Biomark Med 7:517–533. doi:10.2217/bmm.13.77
14. Haas J, Frese KS, Peil B, Kloos W, Keller A, Nietsch R, Feng Z, Muller S, Kayvanpour E, Vogel B, Sedaghat-Hamedani F, Lim WK, Zhao X, Fradkin D, Kohler D, Fischer S, Franke J, Marquart S, Barb I, Li DT, Amr A, Ehlermann P, Mereles D, Weis T, Hassel S, Kremer A, King V, Wirsz E, Isnard R, Komajda M, Serio A, Grasso M, Syrris P, Wicks E, Plagnol V, Lopes L, Gadgaard T, Eiskjaer H, Jorgensen M, Garcia-Giustiniani D, Ortiz-Genga M, Crespo-Leiro MG, Deprez RH, Christiaans I, van Rijsingen IA, Wilde AA, Waldenstrom A, Bolognesi M, Bellazzi R, Morner S, Bermejo JL, Monserrat L, Villard E, Mogensen J, Pinto YM, Charron P, Elliott P, Arbustini E, Katus HA, Meder B (2014) Atlas of the clinical genetics of human dilated cardiomyopathy. Eur Heart J. doi:10.1093/eurheartj/ehu301
15. Hassel D, Dahme T, Erdmann J, Meder B, Huge A, Stoll M, Just S, Hess A, Ehlermann P, Weichenhan D, Grimmler M, Liptau H, Hetzer R, Regitz-Zagrosek V, Fischer C, Nurnberg P, Schunkert H, Katus HA, Rottbauer W (2009) Nexilin mutations destabilize cardiac Z-disks and lead to dilated cardiomyopathy. Nat Med 15:1281–1288. doi:10.1038/nm.2037
16. Hershberger RE, Norton N, Morales A, Li D, Siegfried JD, Gonzalez-Quintana J (2010) Coding sequence rare variants identified in MYBPC3, MYH6, TPM1, TNNC1, and TNNI3 from 312 patients with familial or idiopathic dilated cardiomyopathy. Circ Genetics 3:155–161. doi:10.1161/CIRCGENETICS.109.912345
17. Hershberger RE, Siegfried JD (2011) Update 2011: clinical and genetic issues in familial dilated cardiomyopathy. J Am Coll Cardiol 57:1641–1649. doi:10.1016/j.jacc.2011.01.015
18. Jiao M, Han L, Wang HL, Jin M, Wang XF, Zheng K, Liang YM, Xiao YY (2010) [A long-term follow-up study on the clinical treatment of 75 cases with primary endocardial fibroelastosis]. Zhonghua er ke za zhi. Chin J Pediatr 48:603–609
19. Junqueira LC, Bignolas G, Brentani RR (1979) Picrosirius staining plus polarization microscopy, a specific method for collagen detection in tissue sections. Histochem J 11:447–455
20. Kamisago M, Schmitt JP, McNamara D, Seidman C, Seidman JG (2006) Sarcomere protein gene mutations and inherited heart disease: a beta-cardiac myosin heavy chain mutation causing endocardial fibroelastosis and heart failure. Novart Fdn Symp 274:176–189. doi:10.1002/0470029331.ch11 (**discussion 189–195, 272–176**)
21. Kaufman MH, Bard JBL (1999) The anatomical basis of mouse development. Academic Press Kaufman, London
22. Keller DI, Carrier L, Schwartz K (2002) Genetics of familial cardiomyopathies and arrhythmias. Swiss Med Wkly 132(29–30):401–407
23. Maron BJ, Towbin JA, Thiene G, Antzelevitch C, Corrado D, Arnett D, Moss AJ, Seidman CE, Young JB, American Heart A, Council on Clinical Cardiology HF, Transplantation C, Quality of C, Outcomes R, Functional G, Translational Biology Interdisciplinary Working G, Council on E, Prevention (2006) Contemporary definitions and classification of the cardiomyopathies: an American Heart association scientific statement from the council on clinical cardiology, heart failure and transplantation committee; quality of care and outcomes research and functional genomics and translational biology interdisciplinary working groups; and council on epidemiology and prevention. Circulation 113:1807–1816. doi:10.1161/CIRCULATIONAHA.106.174287
24. Martino TA, Liu P, Sole MJ (1994) Viral infection and the pathogenesis of dilated cardiomyopathy. Circ Res 74:182–188
25. McNally EM, Golbus JR, Puckelwartz MJ (2013) Genetic mutations and mechanisms in dilated cardiomyopathy. J Clin Invest 123:19–26. doi:10.1172/JCI62862
26. Niimura H, Patton KK, McKenna WJ, Soults J, Maron BJ, Seidman JG, Seidman CE (2002) Sarcomere protein gene mutations in hypertrophic cardiomyopathy of the elderly. Circulation 105:446–451
27. Poppe TT, Ferguson HW (2006) Cardiovascular system. In systemic pathology of fish. Scotian Press, London
28. Puchtler H, Waldrop FS, Valentine LS (1973) Polarization microscopic studies of connective tissue stained with picro-sirius red FBA. Beitr Pathol 150:174–187
29. Richardson P, McKenna W, Bristow M, Maisch B, Mautner B, O'Connell J, Olsen E, Thiene G, Goodwin J, Gyarfas I, Martin I, Nordet P (1996) Report of the 1995 World Health Organization/International Society and Federation of Cardiology Task Force on the definition and classification of cardiomyopathies. Circulation 93:841–842
30. Rozengurt N (1994) Endocardial fibroelastosis in common domestic cats in the UK. J Comp Pathol 110:295–301
31. Seki A, Patel S, Ashraf S, Perens G, Fishbein MC (2013) Primary endocardial fibroelastosis: an underappreciated cause of cardiomyopathy in children. Cardiovasc Pathol 22:345–350. doi:10.1016/j.carpath.2013.02.003
32. Wang H, Li Z, Wang J, Sun K, Cui Q, Song L, Zou Y, Wang X, Liu X, Hui R, Fan Y (2010) Mutations in NEXN, a Z-disc gene, are associated with hypertrophic cardiomyopathy. Am J Hum Genet 87:687–693. doi:10.1016/j.ajhg.2010.10.002